Euro. Jnl of Applied Mathematics (1998), *vol.* 9, *pp.* 373–396. Printed in the United Kingdom

Stability of a dislocation: Discrete model

A. B. MOVCHAN[1], R. BULLOUGH[2] and J. R. WILLIS[3]

[1] *School of Mathematical Sciences, University of Bath, Bath BA2 7AY, UK*
[2] *4 Long Meadow, Manor Road, Goring, Reading RG8 9EQ, UK*
[3] *D.A.M.T.P., Silver Street, Cambridge CB3 9EW, UK*

(*Received in revised form 27 February 1998*)

An algorithm, based on a discrete nonlinear model, is presented for evaluation of the critical shear stress required to move a dislocation through a lattice. The stability of solutions of the corresponding evolution problem is analysed. Numerical results provide upper and lower bounds for the critical shear stress.

1 Introduction

The classical linear continuum approach of Taylor [1] and Hirth & Lothe [2] for modelling an edge dislocation in a crystal yields singularities of stress and strain at the dislocation line. An alternative semi-continuum model was constructed by Peierls [3] and Nabarro [4], who assumed a nonlinear discrete sinusoidal interaction between the layers of atoms on each side of the glide plane. In the latter case the strain components are bounded at the dislocation and a defined dislocation core exists. Variations of the simple sinusoidal interatomic force law for the Peierls model were considered by Foreman, Jaswon & Wood [5], and the numerical analysis of the integral equation associated with a vertical array of dislocations was presented by Bullough, Movchan & Willis [6].

A dislocation exists in a discrete atomic lattice, and, therefore, a physical model of such a dislocation should have some correspondence to such a discrete lattice. As the external shear stress reaches a certain critical value (the so-called Peierls stress), the dislocation moves through the lattice. The algorithm for evaluation of the Peierls stress, developed by Nabarro [4], involves a combination of a discrete representation for the misfit energy and a solution of a homogeneous hypersingular integral equation (continuum model).

To obtain the Peierls stress it would be natural to introduce a non-zero constant term (corresponding to an external shear stress) and to solve the non-homogeneous Peierls equation for increasing external shear stress and thereby hope to identify the critical external shear stress for motion of the dislocation (the true Peierls stress). However, the Peierls solution does not allow for small perturbations corresponding to an additional infinitesimal constant term in the equation. This situation explains the reason for Nabarro's choice to use the lattice model for evaluation of the misfit energy and to employ the solution of the homogeneous Peierls equation, to provide the corresponding 'atomic' configuration.

There are many papers on discrete models of dislocations in the physics literature, where the authors observe so-called 'trapping effects' corresponding to the situation when a certain critical load is required to break the resistance of a lattice and to move a dislocation.

One of the simplest approaches corresponds to the discrete one-dimensional model of Frenkel & Kontorova [7], which describes the local interactions between atoms. Hobart [8], for example, performed an equilibrium calculation within the framework of Frenkel and Kontorova, to investigate the modification to the core structure induced by applied stresses. Lombdahl & Srolovitz [9] employed a generalization to two dimensions of the Frenkel–Kontorova model with a molecular dynamics simulation to investigate the nucleation and the motion of dislocations. A limitation of the Frenkel–Kontorova model is its restriction to linear elastic interaction within a single layer of atoms. This precludes consideration of the non-local interactions between these atoms which are associated with the transmission of stress via neighbouring layers. A more rigorous approach would be to allow for nonlinear interactions between atoms, in a fully three-dimensional simulation. Early examples of such calculations are those of Vitek, Perrin & Bowen [10] and Basinski, Duesbery & Taylor [11] (without additional applied stress). During the same period, Basinski, Duesbery & Taylor [12] performed similar equilibrium calculations with allowance for applied stress. The recent work by Carpio *et al.* [13] presents a review of results on dynamics of line singularities; this paper includes examples related to problems of fluid mechanics as well as formulations of dislocation theory.

In the present work we develop a discrete analogue of the Peierls–Nabarro model which describes simply and accurately the nonlinear interaction of two harmonic lattice half-spaces. One of the important issues is the evaluation of the critical stress required to move the dislocation through the lattice and the dependence of the critical stress on the dislocation width (see, for example, Nabarro [4], Foreman, Jaswon & Wood [5] and Hobart [8]). This can be done systematically on the basis of stability analysis of solutions of a certain evolution problem; this approach is different from that employed by Nabarro [4], and it is mathematically rigorous.

We construct discrete lattice models for edge and screw dislocations and use the iteration procedure to obtain the relative displacement across the slip plane. The model allows one to introduce a constant term, corresponding to an external shear stress, directly into the equations. This approach requires a stability analysis for an auxiliary evolution system of nonlinear differential equations. As a result, we obtain lower and upper bounds for the critical shear stress required to move the dislocation through the lattice. Also, we consider the lattice problem for a pair of edge dislocations of opposite sign located on the same glide plane. The lattice model provides an interval for values of an external shear stress associated with a stable equilibrium of this system.

In §2 we give the mathematical formulations of the problem. Having discussed the necessity for the incorporation of discrete components into the model in §3, we proceed in §4 to write down such a model based on discretization and regularization of the Peierls–Nabarro model. Our approach in this section may thus be described as an 'artificial' atomistic model for the dislocation evolution and we find that it does in fact produce interesting predictions for σ_c. In §5 we present numerical results based on the discrete model for different values of the discretization parameter and different types of the force law. We then proceed in §6 to consider a more physically-based discrete model for edge and screw dislocations in which the continuum elasticity of the Peierls–Nabarro theory is replaced by the use of the lattice Green's function. This allows us to make more realistic predictions in §§7 and 8 for σ_c and for the force-velocity law for the dislocations.

2 The governing equations

We deal with a one-dimensional model describing an edge (or screw) dislocation. The magnitude of the Burgers vector is denoted by b. The model of Peierls & Nabarro [3, 4] postulates the relation

$$\sigma(x) = \frac{\mu}{2\pi} \sin\left(\frac{2\pi\Phi(x)}{b}\right) := \frac{\mu}{2\pi} F(\Phi(x), b) \tag{1}$$

between the shear stress $\sigma(x)$ and the difference in displacement $\Phi(x)$ between atoms on either side of the glide plane, assumed to be separated by a distance b. According to this model, the theoretical limit of resistance to shear is the maximum value of $\sigma(x)$, namely,

$$\sigma_t = \frac{\mu}{2\pi}.$$

The model envisages two elastic half-spaces joined by a continuous distribution of elastic springs modelled by Eq. (1). Equilibrium in the absence of other forces then requires that Φ should satisfy the hypersingular integral equation

$$F(\Phi(x), b) = -\frac{1}{1-\nu} \int_{-\infty}^{\infty} \frac{\Phi(x')}{(x-x')^2} \mathrm{d}x', \tag{2}$$

where ν is the Poisson ratio; $F(s, b)$ is as defined in Eq. (1) but, more generally, could be taken as any b-periodic function of s, chosen to represent the interatomic force law. The same equation describes a screw dislocation, if the factor $(1-\nu)^{-1}$ is omitted. Equation (2), and succeeding equations, are normalized so that stress is measured in units of the theoretical limit of resistance to shear σ_t; thus, the physical stress corresponding to F is[1] $\sigma_t F$. The integral in Eq. (2) is defined in the Hadamard finite part sense. The solution of Eqs. (2), (1), employed in Nabarro [4], has the explicit form

$$\Phi(x) = -\frac{b}{\pi} \tan^{-1} \frac{2(1-\nu)\, x}{b}. \tag{3}$$

It is evident that the solution is not unique. For example, any constant $bk/2$, where k is an integer, also satisfies Eqs. (2), (1). The distinctive property of the solution (3) is that $\Phi(x)$ is monotonic and

$$\Phi(-\infty) > 0, \quad \Phi(\infty) < 0, \quad \Phi(-\infty) - \Phi(\infty) = b. \tag{4}$$

To move the dislocation through the crystal lattice one has to apply an external shear stress. In accordance with Nabarro [4], the Peierls critical stress is specified by

$$\sigma_c = \max_{\alpha} \left[-\frac{1}{b^2} \frac{\mathrm{d}E}{\mathrm{d}\alpha}(\alpha) \right], \tag{5}$$

where

$$E = \frac{b^2\mu}{8\pi^2} \sum_{n=-\infty}^{\infty} G[-2\pi\, \Phi[(\alpha + n/2)\, b]] \tag{6}$$

[1] This normalization was originally introduced by Peierls and Nabarro, and is adopted here for consistency with their work.

https://doi.org/10.1017/S0956792598003489 Published online by Cambridge University Press

is the varying part of the misfit energy associated with the dislocation, which moves through the distance αb, and

$$G(x) = \frac{2\pi}{b}\int_0^x F(s,b)\,\mathrm{d}s. \tag{7}$$

For the sinusoidal law (1) the quantity (5) is evaluated (see Nabarro [4]) in the form

$$\sigma_c = \frac{2\mu}{1-\nu}\mathrm{e}^{-\frac{2\pi}{1-\nu}}, \tag{8}$$

where μ is the shear modulus. In particular, for $\nu = 0.3$

$$\sigma_c = 3.6\times 10^{-4}\,\mu, \tag{9}$$

which gives a small (but non-zero) value for the critical shear stress required to move the dislocation through the lattice.

We note that the solution Φ of the continuum model is used in the discrete approximation (6) of the misfit energy.

To evaluate the critical (Peierls) stress necessary to move the dislocation, one could try to modify the scheme adopted by Peierls and Nabarro, and consider the non-homogeneous equation

$$\sigma + (1-\nu)\,F(\Phi(x),b) = -\int_{-\infty}^{\infty}\frac{\Phi(x')}{(x-x')^2}\,\mathrm{d}x', \quad 0<\sigma\ll 1. \tag{10}$$

If $\Phi(x) = \Phi^*$, constant, the integral in Eq. (10) vanishes, and therefore $\Phi = \Phi^*$ is a solution of Eq. (10), if

$$\sigma + (1-\nu)\,F(\Phi^*,b) = 0.$$

The function F is assumed to be periodic (with period b) with respect to its first argument, and we remark that the Eq. (10) has an infinite set of constant solutions (since $|\sigma|\ll 1$). However, if we assume that Φ satisfies simultaneously the conditions (4), then all constant solutions will be eliminated. It turns out (see §3) that for any positive σ the problem (10), (4) does not have a solution, and, therefore, the continuum model for a non-homogeneous equation cannot be used for evaluation of the critical Peierls stress.

In the present work, we propose an alternative discrete model and evaluate upper and lower bounds for the critical load. Namely, instead of a continuous function Φ we introduce an array of values associated with the displacement jump function evaluated on a countable set, and the hypersingular integral (in the right-hand side of Eq. (2)) is approximated by a series. In addition, Φ is assumed to depend on the time-like variable t, and a stabilization algorithm is employed to obtain a solution. The objective is to study the stability of an edge dislocation in a discrete lattice. The following non-homogeneous system of nonlinear differential equations is introduced for the displacement jump $\Phi(x_j,t)$ on the glide plane:

$$\frac{\partial}{\partial t}\Phi(x_j,t) = \sigma + (1-\nu)\,F(\Phi(x_j,t),b) + \sum_{i=-n+1}^{n} a(x_i,x_j)\,\Phi(x_i,t), \tag{11}$$

$$j = 1,\ldots,n, \quad n\gg 1,$$

where x_j is an element of a discrete set of points on the slip line, and the coefficients

https://doi.org/10.1017/S0956792598003489 Published online by Cambridge University Press

$a(x_i, x_j)$ are specified below (see §4). For any $t > 0$ the jump function Φ is subjected to the following conditions specified at the ends of a large interval

$$\Phi(-n+1, t) > 0, \quad \Phi(n, t) < 0. \tag{12}$$

The constant term σ in Eq. (11) characterizes the applied shear stress.

3 The continuum approach

Here we consider the classical continuum model for a single dislocation and show that it is essential that the Peierls–Nabarro algorithm deals with a homogeneous hypersingular integral equation. Any attempt to introduce an additional non-zero constant term fails: the dislocation becomes unstable and moves through the lattice.

3.1 The solution (3) is unstable

It is shown here that for any non-zero infinitesimal σ a solution of Eq. (10) fails to satisfy conditions (4).

Let Φ_0 denote a function, which satisfies the homogeneous Eq. (10) ($\sigma = 0$) and conditions (4) specified at infinity. Assume that for small values of $\sigma > 0$ there exists a function

$$\Phi = \Phi_0 + \sigma \Phi_1 + O(\sigma^2) \tag{13}$$

that also satisfies Eqs. (10), (4). The term $\sigma \Phi_1$ represents a small smooth perturbation. Then the following asymptotic equality holds:

$$\sigma + (1-\nu)\left(F(\Phi_0(x), b) + \frac{\mathrm{d}}{\mathrm{d}\Phi} F(\Phi_0(x), b)\, \sigma \Phi_1(x) + O(\sigma^2)\right)$$
$$= -\left\{ \int_{-\infty}^{\infty} \frac{\Phi_0(x')}{(x-x')^2}\,\mathrm{d}x' + \sigma \int_{-\infty}^{\infty} \frac{\Phi_1(x')}{(x-x')^2}\,\mathrm{d}x' \right\}.$$

For terms of order $O(\sigma)$ we obtain

$$1 + (1-\nu)\,\Phi_1(x) \frac{\mathrm{d}}{\mathrm{d}\Phi} F(\Phi_0(x), b) = -\int_{-\infty}^{\infty} \frac{\Phi_1(x')}{(x-x')^2}\,\mathrm{d}x'. \tag{14}$$

The Eq. (14) can be multiplied by $\Phi_0'(x)$ and then integrated over $(-\infty, \infty)$, to give

$$\int_{-\infty}^{\infty} \Phi_0'(x)\,\mathrm{d}x + (1-\nu) \int_{-\infty}^{\infty} \Phi_1(x)\,\Phi_0'(x) \frac{\mathrm{d}F}{\mathrm{d}\Phi}(\Phi_0(x))\,\mathrm{d}x$$
$$= -\int_{-\infty}^{\infty} \Phi_0'(x)\,\mathrm{d}x \int_{-\infty}^{\infty} \frac{\Phi_1(x')}{(x-x')^2}\,\mathrm{d}x'.$$

This yields

$$[\Phi_0(x)]_{-\infty}^{\infty} + (1-\nu) \int_{-\infty}^{\infty} \Phi_1(x) \frac{\mathrm{d}F}{\mathrm{d}x}(\Phi_0(x))\,\mathrm{d}x = \int_{-\infty}^{\infty} \Phi_1'(x')\,\mathrm{d}x' \int_{-\infty}^{\infty} \frac{\Phi_0'(x)}{x-x'}\,\mathrm{d}x.$$

Taking into account Eq. (2) (with respect to Φ_0) and integrating by parts, we obtain

$$[\Phi_0(x)]_{-\infty}^{\infty} = 0$$

which contradicts (4). Thus, the assumption (13) is not valid. In other words, if we follow

https://doi.org/10.1017/S0956792598003489 Published online by Cambridge University Press

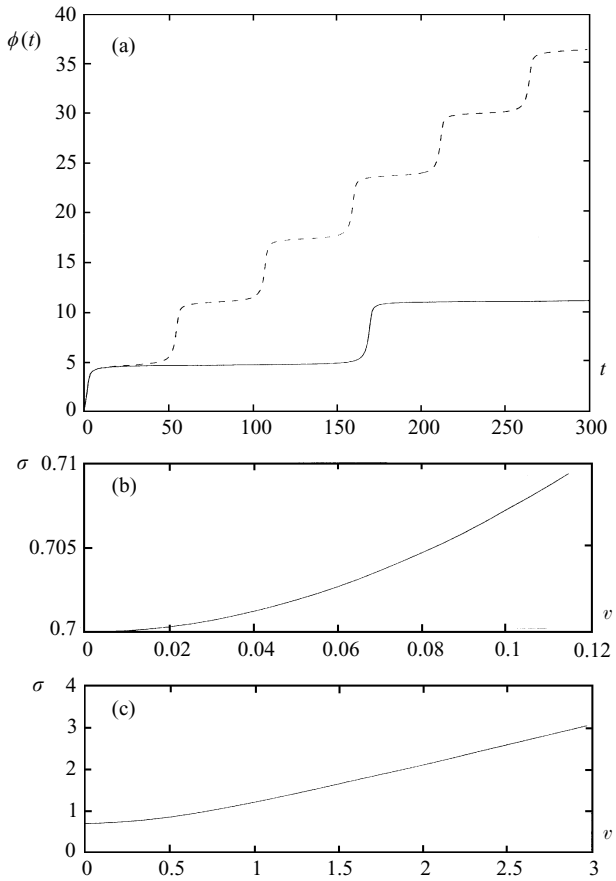

FIGURE 1. (a) Solutions of the equation $\phi_{,t} = 0.7 \sin \phi + \sigma$ for the cases when $\sigma = 0.701$ (solid line) and $\sigma = 0.71$ (dashed line). These curves oscillate about straight lines; the slope of these lines is denoted by v; (b) the plot of σ versus v for small values of v; (c) the plot of σ versus v for larger values of v.

the continuum approach and introduce even an infinitesimal additional constant term in the equation, no equilibrium solutions adjacent to the Peierls solution (corresponding to zero applied stress) exist. This is why Nabarro [4] injected a partial discretization into his evaluation of critical stress. Equation (6) estimates the energy of the dislocation due to interaction between atoms on either side of the slip plane, situated at points whose x-coordinates are integers multiplied by $b/2$. The solution $\Phi(x)$ of the continuum Eq. (2) was employed to approximate the relative separation of atoms, whether in or out of equilibrium.

3.2 The evolution model

Now assume that $\Phi = \Phi(x, t)$ with t being the time-like variable, and instead of Eq. (10) consider

$$\frac{\partial}{\partial t}\Phi(x,t) = \int_{-\infty}^{+\infty} \frac{\Phi(x',t)\,\mathrm{d}x'}{(x-x')^2} + (1-\nu)\,F(\Phi(x,t),b) + \sigma, \quad \sigma > 0. \tag{15}$$

https://doi.org/10.1017/S0956792598003489 Published online by Cambridge University Press

Also, assume that

$$\Phi(x,0)=\Phi_0, \tag{16}$$

where Φ_0 satisfies the homogeneous Eq. (10) and the conditions (4). The results of numerical calculations show (consistently with §3.1) that for any positive σ

$$\Phi(x,t)\to\Phi^* \quad \text{as} \quad t\to\infty, \tag{17}$$

where Φ^* represents a *constant solution* of the equation

$$(1-\nu)\,F(\Phi^*,b)+\sigma=0, \tag{18}$$

provided the latter is solvable. Physically it means that the dislocation has moved to infinity. To illustrate this, we refer to Fig. 7, which shows the dislocation motion for the case of the discrete model.

We note that if Eq. (18) does not have real roots, then the x-independent solution of the equation

$$\frac{\partial}{\partial t}\tilde{\Phi}=\alpha\,F(\tilde{\Phi},b)+\sigma, \tag{19}$$

$$\alpha=(1-\nu),$$

diverges as $t\to\infty$.

For the purpose of illustration, we analyse the behaviour of the solution of the evolution Eq. (19) when $t\to\infty$ and when σ is sufficiently large. The reader should not regard this simple example as a physical model. Consider the case when the function F is given by Eq. (1) with $b=2\pi$, so that

$$F=F(\tilde{\Phi}(t))=\sin\tilde{\Phi}(t),$$

and let $\nu=0.3$. We also assume that $\tilde{\Phi}(0)=\beta$. The solution $\tilde{\Phi}$ of Eq. (19) admits the following explicit form:

$$\tilde{\Phi}(t)=2\tan^{-1}\frac{1}{\sigma}\left\{-\alpha+\sqrt{\sigma^2-\alpha^2}\tan\left(\frac{(1+C_k)}{2}\sqrt{\sigma^2-\alpha^2}\right)\right\}$$
$$+2\pi(l_0+k), \quad t\in(t_{k-1},t_k), \quad k=0,1,2,\ldots, \tag{20}$$

where

$$t_k=\frac{1}{\sqrt{\sigma^2-\alpha^2}}\left\{\pi(2k+1)-2\tan^{-1}\left\{\frac{\sigma\tan(\beta/2)+\alpha}{\sqrt{\sigma^2-\alpha^2}}\right\}\right\}, \quad k\geqslant 0; \quad t_{-1}=0,$$

$$C_k=\pi(\sigma^2-\alpha^2)^{-1/2}-t_k,$$

and the integer constant l_0 is specified by

$$l_0=[(2\pi)^{-1}\,|\beta-2\tan^{-1}(\tan(\beta/2))|].$$

The graphs of the solution of Eq. (19) are given in Fig. 1(a) for the cases when $\sigma=0.701$ and $\sigma=0.71$, taking the initial value $\beta=0$. We observe that the solution tends to infinity

https://doi.org/10.1017/S0956792598003489 Published online by Cambridge University Press

as $t \to +\infty$ and oscillates about some straight line.[2] The frequency of oscillation increases for bigger values of σ, and the slope increases too when σ is growing (see Fig. 1(b)).

Later in the text a discrete operator of convolution type will be introduced instead of the integral operator (see Eq. (10)), and the critical value of σ producing unstable solutions will be evaluated. We shall see that the shape of the 'dislocation trajectory' in the lattice looks similar to one presented in Fig. 1(a), but due to the presence of the operator of convolution type, the values of the critical load will be much smaller than those given in the above elementary example.

4 Discretization

Let x_j, $j = -n+1, \dots, n$ be nodes uniformly distributed on the interval $(-a, a)$; $N = 2n$ denotes the total number of points. The following notation is adopted:

$$\Phi_j(t) = \Phi(x_j, t),$$

where t is the time-like variable. The value $b = 1$ is used for the interatomic space parameter (the modulus of Burgers vector) in all calculations.

We consider a system of differential equations

$$\frac{\partial}{\partial t}\boldsymbol{\Phi} = \mathbf{L}\boldsymbol{\Phi} + \mathcal{N}\boldsymbol{\Phi} + \Sigma^2 \mathbf{I}. \tag{21}$$

Here $\sigma = \Sigma^2 \neq 0$ specifies the external load, $\mathbf{I}$ is the identity matrix, the vector $\boldsymbol{\Phi}$ is defined by

$$\boldsymbol{\Phi} = (\Phi_{-n+1}, \Phi_{-n+2}, \dots, \Phi_{n-1}, \Phi_n)^{\mathrm{T}};$$

the operator $\mathbf{L}$ is linear, and $\mathcal{N}$ is a nonlinear diagonal matrix function.

4.1 The linear part: regularization

The linear operator $\mathbf{L}$ is specified as follows:

$$(\mathbf{L}\boldsymbol{\Phi})_j = m \sum_{i=-n+1}^{n} \mathcal{K}(i-j, \mu_*, \lambda_*)\, \Phi_i + \sum_{\pm} m R_{\pm}^{(j)}, \tag{22}$$

where m is the discretization parameter (in particular, $m = 2$ corresponds to a half-integer step of the discretization). The function $\mathcal{K}$ is defined by the equality

$$\mathcal{K}(\xi; \alpha, \beta) = \frac{\xi^2 - \alpha^2}{(\xi^2 + \beta^2)^2}. \tag{23}$$

The parameters λ_*, μ_* satisfy the relation

$$\mu_*^2 = \left\{ \sum_{i=-3n+1}^{3n} \frac{1}{(i^2 + \lambda_*^2)^2} \right\}^{-1} \sum_{i=-3n+1}^{3n} \frac{i^2}{(i^2 + \lambda_*^2)^2}. \tag{24}$$

[2] The reader should not regard this simple example as a physical model. It is presented for the purpose of illustration, so that one can see the behaviour of the solution of the evolution Eq. (19) when $t \to \infty$ and when σ is sufficiently large.

https://doi.org/10.1017/S0956792598003489 Published online by Cambridge University Press

It will be shown later in the text that the function (23) enables one to approximate the stress produced on the x-axis by the lattice Green's function. The choice of the parameters λ_*, μ_* is made in such a way that the operator $\mathbf{L}$ applied to a constant vector gives zero. The terms $R_{\pm}^{(j)}$ take into account the asymptotic behaviour of the solution at infinity.

The correction terms at the ends of the interval $(-a, a)$ are

$$R_{+}^{(j)} = \Phi_n \sum_{i=n+1}^{3n} \frac{(i-j)^2-\mu_*^2}{((i-j)^2+\lambda_*^2)^2},$$

$$R_{-}^{(j)} = \Phi_{-n+1} \sum_{i=-3n+1}^{-n} \frac{(i-j)^2-\mu_*^2}{((i-j)^2+\lambda_*^2)^2}. \tag{25}$$

Thus, $\mathbf{L}\boldsymbol{\Phi}$ gives a discrete analogue of the finite-part integral in Eq. (2). In particular,

$$\mathbf{L}\boldsymbol{\Phi} = 0,$$

for any constant $\boldsymbol{\Phi}$, and in addition we note that

$$-\frac{1}{\pi}\mathscr{K}(\xi;\alpha,\alpha) = \mathscr{F}[|x|\,\mathrm{e}^{-\alpha|x|};\xi], \tag{26}$$

where

$$\mathscr{F}[f(x);\xi] = \frac{1}{2\pi}\int_{-\infty}^{\infty} f(x)\,\mathrm{e}^{ix\xi}\,\mathrm{d}x$$

denotes the Fourier transform. The presence of the exponentially decaying factor in Eq. (26) corresponds to the regularization of

$$-\frac{1}{\pi\xi^2} = \mathscr{F}[|x|;\xi],$$

wher the right-hand side is defined in terms of distributions (compare with the Debye cut-off procedure [14]).

4.2 The nonlinear part; stability of the solution

The nonlinear part $\mathscr{N}\boldsymbol{\Phi}$ for the discretized system (21) is defined by the equality

$$(\mathscr{N}\boldsymbol{\Phi})_j = (1-\nu)\,F(2\pi\Phi_j), \tag{27}$$

where F is a 1-periodic smooth function.

We are looking for a vector function which satisfies the following condition at infinity:

$$\mathrm{sign}(\Phi_n(t)\,\Phi_{-n+1}(t)) = -1 \quad \text{as} \quad t\to\infty. \tag{28}$$

Suppose that $\partial/\partial t\,\boldsymbol{\Phi}\to 0$ as $t\to\infty$. Then in the limit we obtain a vector function, which satisfies the system

$$\mathbf{L}\boldsymbol{\Phi} + \mathscr{N}\boldsymbol{\Phi} + \Sigma^2\mathbf{I} = 0. \tag{29}$$

https://doi.org/10.1017/S0956792598003489 Published online by Cambridge University Press

Consider the following evolution system:

$$\begin{cases} \dfrac{\partial}{\partial t}\boldsymbol{\Phi} = \mathscr{A}\boldsymbol{\Phi} + \Sigma^2 \mathbf{I}, \\ \dfrac{\partial}{\partial t}\Sigma = 0, \end{cases} \tag{30}$$

where

$$\mathscr{A}\boldsymbol{\Phi} = \mathbf{L}\boldsymbol{\Phi} + \mathscr{N}\boldsymbol{\Phi}.$$

The vector $\boldsymbol{\Phi}^{(0)}$ is assumed to be a non-trivial solution of the homogeneous system

$$\mathscr{A}\boldsymbol{\Phi}^{(0)} = 0, \tag{31}$$

and to satisfy the conditions

$$\lim_{K\to\infty} [\Phi_j^{(0)}]_{j=-K}^{j=K} = b, \quad \operatorname{sign}(\Phi_{-K}^{(0)}\Phi_K^{(0)}) = -1 \quad \text{for} \quad K \gg 1. \tag{32}$$

For small Σ we use the representation

$$\boldsymbol{\Phi} = \boldsymbol{\Phi}^{(0)} + \boldsymbol{\Psi}, \quad \|\boldsymbol{\Psi}\| \ll 1,$$

and analyse stability of the zero solution of the system

$$\begin{cases} \dfrac{\partial}{\partial t}\boldsymbol{\Psi} = \mathbf{L}\boldsymbol{\Psi} + \dfrac{D\mathscr{N}}{D\boldsymbol{\Phi}}(\boldsymbol{\Phi}^{(0)})\,\boldsymbol{\Psi} + \Sigma^2\mathbf{I} + \mathbf{H}(\boldsymbol{\Psi}), \\ \dfrac{\partial}{\partial t}\Sigma = 0, \end{cases} \tag{33}$$

where

$$\mathbf{H}(\boldsymbol{\Psi}) = \mathscr{N}(\boldsymbol{\Phi}^{(0)} + \boldsymbol{\Psi}) - \frac{D\mathscr{N}}{D\boldsymbol{\Phi}}(\boldsymbol{\Phi}^{(0)})\,\boldsymbol{\Psi} - \mathscr{N}(\boldsymbol{\Phi}^{(0)}) = O(\|\boldsymbol{\Psi}\|^2) \quad \text{as} \quad \|\boldsymbol{\Psi}\| \to 0.$$

Our numerical calculations show that there exists a solution $\boldsymbol{\Phi}^{(0)}$ of the discrete homogeneous model such that the matrix of the linearized system has *one zero eigenvalue*, and *other eigenvalues are negative*.

In terms of Carr [15], the system (33) has a one-dimensional centre manifold defined by the equality

$$\boldsymbol{\Psi} = g(\Sigma), \tag{34}$$

where g is to be determined. We introduce the operator

$$\mathscr{M}(\boldsymbol{\Psi}, \Sigma) = \mathbf{L}\boldsymbol{\Psi} + \frac{D\mathscr{N}}{D\boldsymbol{\Phi}}(\boldsymbol{\Phi}^{(0)})\,\boldsymbol{\Psi} + \Sigma^2\mathbf{I} + \mathbf{H}(\boldsymbol{\Psi})$$

and observe that if

$$\boldsymbol{\Psi} = -\left[\mathbf{L} + \frac{D\mathscr{N}}{D\boldsymbol{\Phi}}(\boldsymbol{\Phi}^{(0)})\right]^{-1} \Sigma^2\mathbf{I},$$

then

$$\|\mathscr{M}\boldsymbol{\Psi}\| = O(\Sigma^4).$$

https://doi.org/10.1017/S0956792598003489 Published online by Cambridge University Press

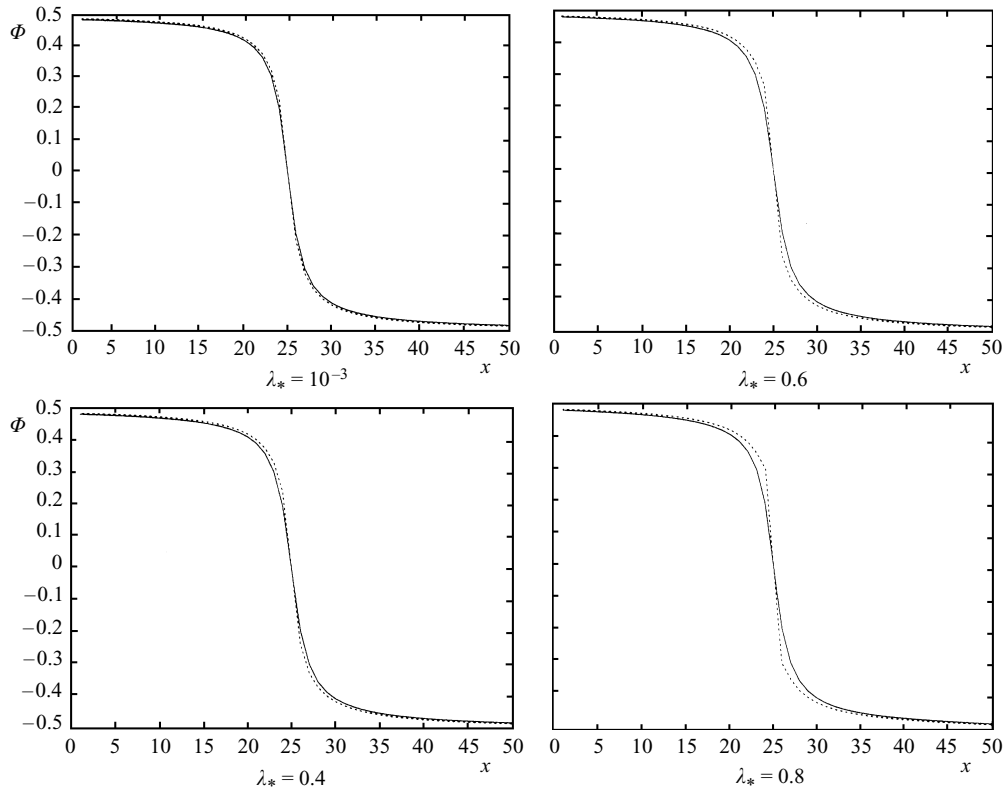

FIGURE 2. Solutions of the homogeneous problem with the sinusoidal force law (we assume zero external stress). The solid line corresponds to the semi-continuum model solution; the dashed line shows the discrete model solution.

We obtain that

$$g(\Sigma) = -\left[\mathbf{L} + \frac{D\mathcal{N}}{D\boldsymbol{\Phi}}(\boldsymbol{\Phi}^{(0)})\right]^{-1} \Sigma^2 \mathbf{I} + O(\Sigma^4),$$

and the equation that governs stability of the zero solution of the system (33) is

$$\frac{\partial \Sigma}{\partial t} = 0.$$

This proves that the zero solution of the system (33) is stable.

In the next section we discuss numerical results obtained in accordance with the stabilization algorithm applied to the discrete model.

5 Numerical results for the case of small λ_*

We would like to obtain bounds for the critical load required to move the edge dislocation through the lattice, and to compare our results with those presented by Peierls & Nabarro [3, 4].

https://doi.org/10.1017/S0956792598003489 Published online by Cambridge University Press

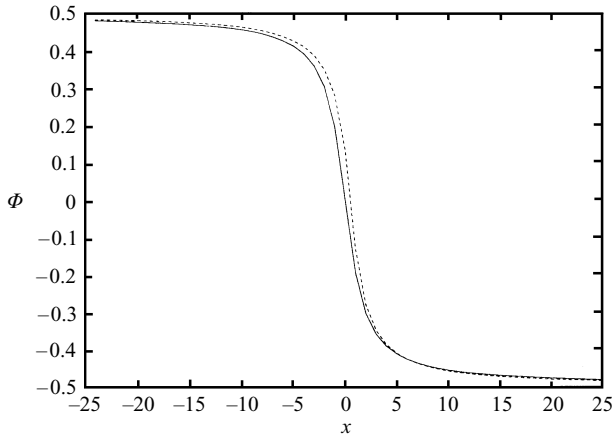

FIGURE 3. The stable equilibrium solution (dashed line) and the unstable equilibrium solution (solid line) for the sinusoidal force law.

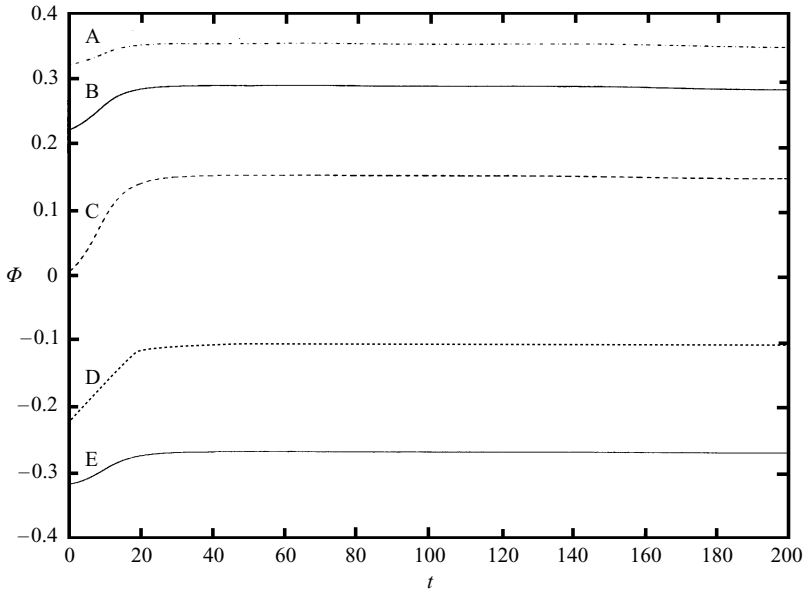

FIGURE 4. The displacement jump versus time calculated for the sinusoidal force law at five points on the glide line: $A = (-1.0, 0)$, $B = (-0.5, 0)$, $C = (0, 0)$, $D = (0.5, 0)$, $E = (1.0, 0)$; $\sigma = 2.0 \cdot 10^{-3}$.

5.1 Comparison with the continuum model

Let the function F, describing the interatomic force law, have the form

$$F(s) = \sin(2\pi s),$$

as in the Peierls model [3]. Equilibrium solutions of the discrete model (21) must satisfy (29). First, we note that the relative displacement across the glide plane, obtained by solving (21) with $\sigma = \Sigma^2 = 0$, is different from Eq. (3). In Fig. 2 we present the numerical solution for

https://doi.org/10.1017/S0956792598003489 Published online by Cambridge University Press

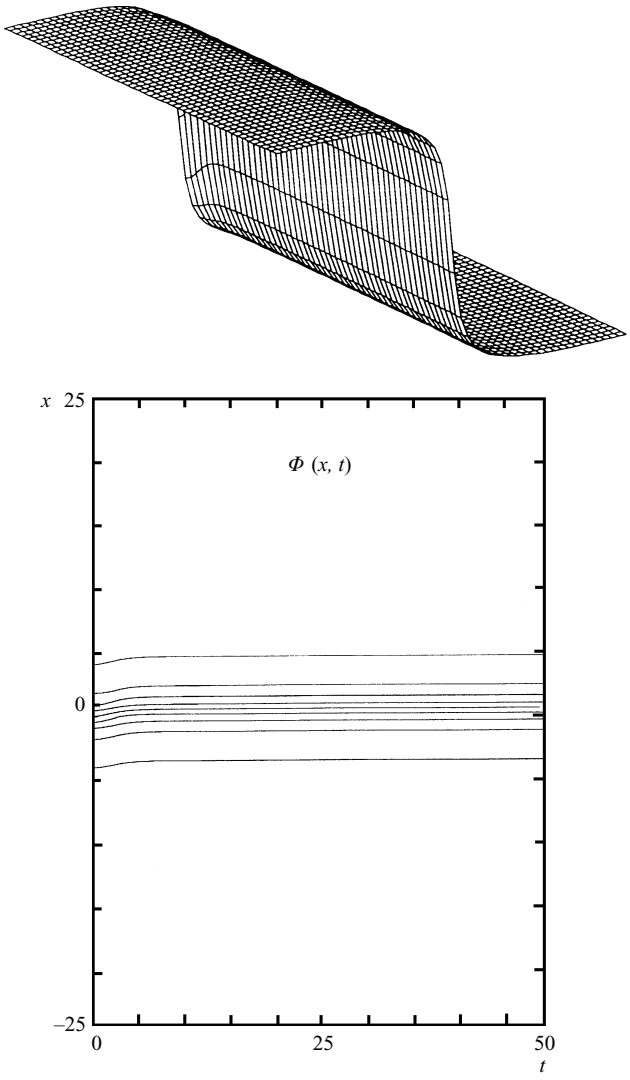

FIGURE 5. The displacement jump as a function of x and t for the sinusoidal force law; $\sigma = 2.0 \cdot 10^{-3}$ (contour lines and the corresponding three-dimensional surface).

different values of $\lambda_* > 0$, with the symmetry $\Phi_{-j} = \Phi_j$ imposed. This solution was obtained using the NAG subroutine C05NBF (the Newton–Raphson method). It turns out that as λ_* increases we obtain the greater discrepancy between Eq. (3) and the solution $\boldsymbol{\Phi}^{(0)}$ associated with the discrete model. On the other hand, when λ_* is decreasing, the discrepancy tends to some non-zero quantity which depends on the discretization parameter m (see Eq. (22)). In the stability analysis, presented here, we use $\lambda_* = 10^{-2}$, $m = 2$. In all calculations we assume that the Poisson ratio ν is equal to 0.3. We deliberately use the half-integer step of discretization to make the numerical scheme close enough to the model of Nabarro [4].

https://doi.org/10.1017/S0956792598003489 Published online by Cambridge University Press

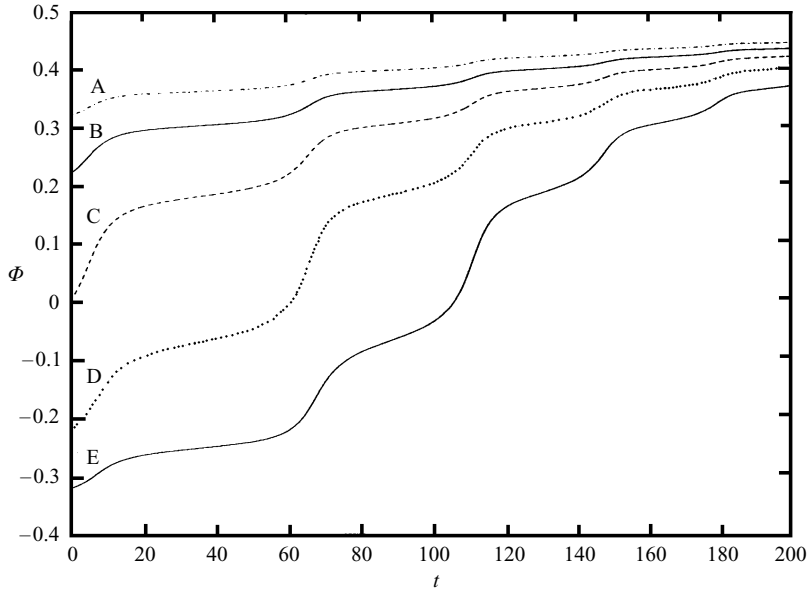

FIGURE 6. The displacement jump versus time for the sinusoidal force law; $\sigma = 4.0 \cdot 10^{-3}$.

5.2 Stability of solutions of the discrete model

We are looking for a stable equilibrium solution $\boldsymbol{\Phi}^{(0)}$ associated with the discrete model. First, for the sinusoidal force law we find that the skew-symmetric solution, which is close to Eq. (3), is unstable. Numerical results show that the Jacobi matrix

$$\mathbf{J} = \mathbf{L} + \frac{D\mathcal{N}}{D\boldsymbol{\Phi}}(\boldsymbol{\Phi}^{(0)}) \tag{35}$$

has one positive eigenvalue, other eigenvalues being negative.

However, the solution is not unique. There exists another solution of the discrete problem, which satisfies the required conditions at infinity, and it is stable. Numerically it can be traced by C05NBF as well as by the stabilization algorithm based on the solution of Eq. (21) by Euler's method. Both solutions are presented in Fig. 3. In the vicinity of the origin the curve corresponding to the stable solution is shifted by a half-step of discretization with respect to the unstable one.

Now we estimate the bounds for the critical shear stress required to move the edge dislocation through the lattice. For the sinusoidal force law and applied load with $\sigma = 2.0 \cdot 10^{-3}$ we obtain (see Figs. 4 and 5) that as $t \to \infty$ the solution of Eqs. (22), (28) tends to the stable equilibrium solution (all eigenvalues of the corresponding Jacobi matrix are negative). In Fig. 4 we show the evolution of the displacement jump at five points on the glide plane. Also, for the qualitative description of the evolution process it is helpful to have the three-dimensional surface and contour line pictures presented in Fig. 5. The contour lines show that, as $t \to \infty$, the high-gradient region associated with the dislocation core moves through a finite distance (as $t \to \infty$, the slope of the contour lines tends to zero). The numerical results show that the eigenvalues of the Jacobi matrix (35), evaluated on this

https://doi.org/10.1017/S0956792598003489 Published online by Cambridge University Press

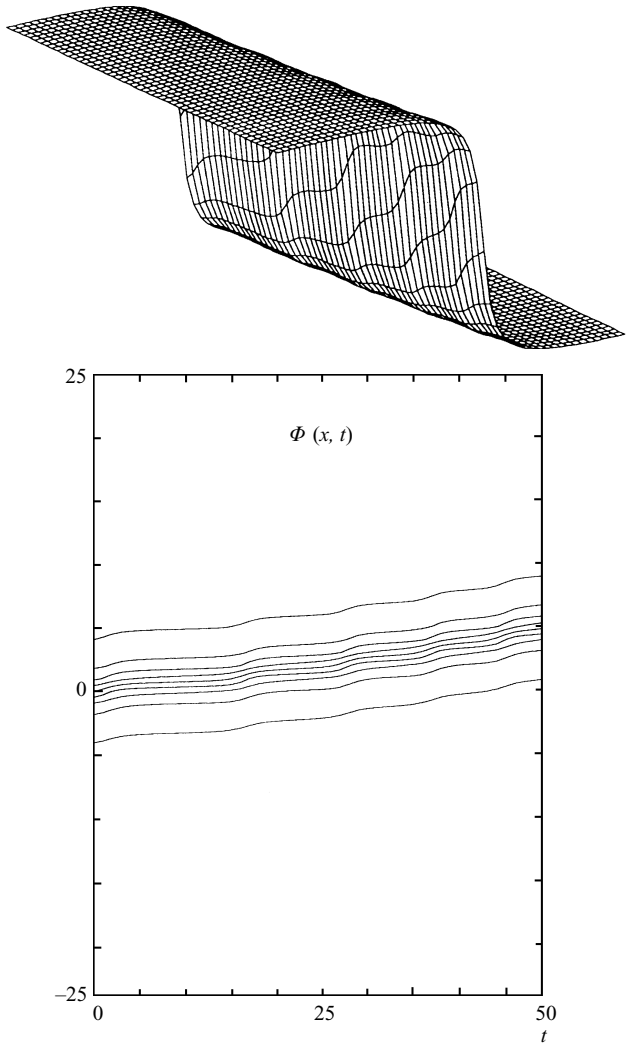

FIGURE 7. The displacement jump as a function of x and t; $\sigma = 4.0 \cdot 10^{-3}$ for the sinusoidal force law (contour lines and the corresponding three-dimensional surface).

equilibrium solution, are negative, and therefore this solution is stable. Hence $\sigma = 2.0 \cdot 10^{-3}$ provides a lower bound for critical shear load.

When σ is increased to $4.0 \cdot 10^{-3}$ the dislocation changes its position in the lattice. In Fig. 6 we show the curves corresponding to the displacement jump versus time at five particular points on the glide plane. As $t \to \infty$ these curves approach the horizontal line which corresponds to the constant solution of Eq. (31). In Fig. 7 one can see the nonzero slope between the contour lines and the time-axis. The dislocation moves rigidly through the lattice, and the value $\sigma = 4.0 \cdot 10^{-3}$ gives an upper bound for the shear load. We remark that the bounds, obtained here and the Peierls stress (9) have the same order of the magnitude.

https://doi.org/10.1017/S0956792598003489 Published online by Cambridge University Press

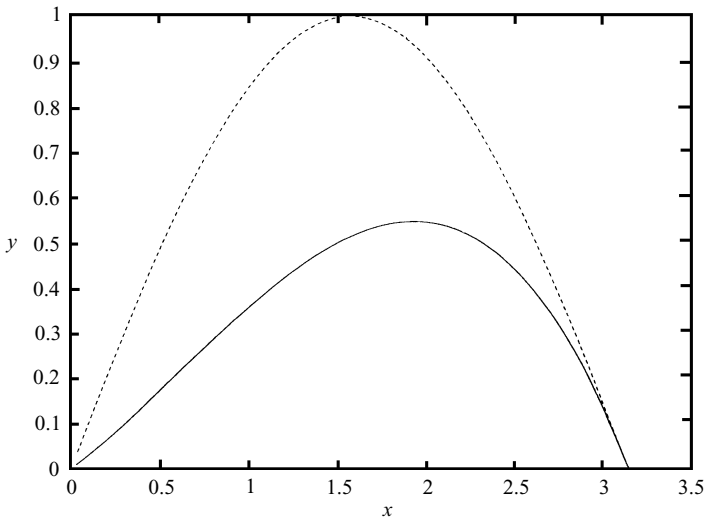

FIGURE 8. Two types of the interatomic force law: $y = \sin x$ (dashed line), $y = (\pi - x)\, x(0.3\pi + 0.7x)/\pi^2$ (solid line).

5.3 Modified force law

Consider a different force law, shown in Fig. 8. The function F is assumed to be 1-periodic, and its restriction to the interval $(-1/2, 1/2]$ is defined by

$$F(s) = \begin{cases} r(2\pi s), & 0 \leqslant s \leqslant 1/2 \\ -r(-2\pi s), & -1/2 < s < 0, \end{cases} \tag{36}$$

where

$$r(x) = \frac{1}{\pi^2}(\pi - x)\, x(0.3\pi + 0.7x).$$

The plot of this function has the same slope as $\sin(x)$ at the right end of the interval $(0, \pi]$ (these force laws provide the same resistance to shear at infinity). At the origin the slope has been decreased. We refer to Foreman *et al.* [5], and note that it corresponds to a more realistic physical model than one with the sinusoidal force law.

Calculations (still with $\lambda_* = 10^{-2}$) similar to those performed for the sinusoidal law show that, when $\sigma = 10^{-4}$, there is a stable equilibrium solution, while for $\sigma = 10^{-3}$ the long-time behaviour corresponds to motion of the dislocation. The critical stress thus lies within the interval $(10^{-4}, 10^{-3})$, so that the force law (36) gives a smaller critical stress than the sinusoidal law.

6 Lattice calculations

It was shown in the previous section that for small values of the parameter λ_* the solution of the discretized problem is close to the continuum solution (3). A half-integer step of the discretization, consistent with Nabarro's approach, provides bounds for the critical shear stress, which have the same order of magnitude as the Peierls stress evaluated explicitly in Nabarro [4]. Nevertheless, these small values of the parameter λ_* are, probably, different from those describing a discrete lattice.

https://doi.org/10.1017/S0956792598003489 Published online by Cambridge University Press

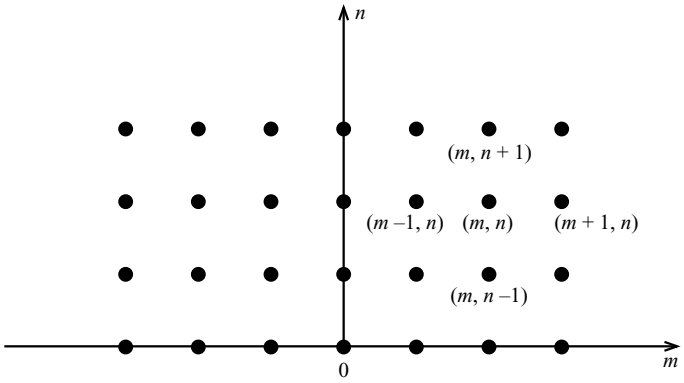

FIGURE 9. A periodic square lattice in a half-plane.

6.1 Lattice Green's function

In this section we consider a linear discrete model for the case of anti-plane shear in a half-plane with the Dirichlet boundary condition. The body force density is assumed to be zero. For a square lattice with $b = 1$ (see Fig. 9) we assume that the boundary point $(0, 0)$ is moved in the transversal direction; all other boundary points are kept fixed.

Let $w_{m,n}$ denote a displacement of an internal point with coordinates (m, n), where m and n are integer. Assuming only nearest-neighbour interactions in the harmonic, or linear, approximation, the equilibrium equation has the form

$$w_{m+1,n} + w_{m-1,n} + w_{m,n+1} + w_{m,n-1} - 4w_{m,n} = 0, \quad n \geqslant 1, \tag{37}$$

and the boundary condition is

$$w_{m,0} \equiv F_m = \delta_{m,0}. \tag{38}$$

The displacement is assumed to decay at infinity

$$w_{m,n} \to 0, \quad m^2 + n^2 \to \infty. \tag{39}$$

We use the discrete Fourier transform with respect to m and obtain the following recurrence relation

$$\tilde{w}(t, n-1) + \tilde{w}(t, n+1) - 2\tilde{w}(t, n) + 2(\cos t - 1)\,\tilde{w}(t, n) = 0, \quad n > 1, \tag{40}$$

and the boundary condition

$$\tilde{w}(t, 0) = \tilde{F}(t). \tag{41}$$

The condition at infinity has the form

$$\tilde{w}(t, n) \to 0, \quad \text{as} \quad n \to \infty. \tag{42}$$

Here

$$\tilde{w}(t, n) = \sum_m w_{m,n}\, \mathrm{e}^{imt},$$

$$\tilde{F}(t) = \sum_m F_m\, \mathrm{e}^{imt}.$$

https://doi.org/10.1017/S0956792598003489 Published online by Cambridge University Press

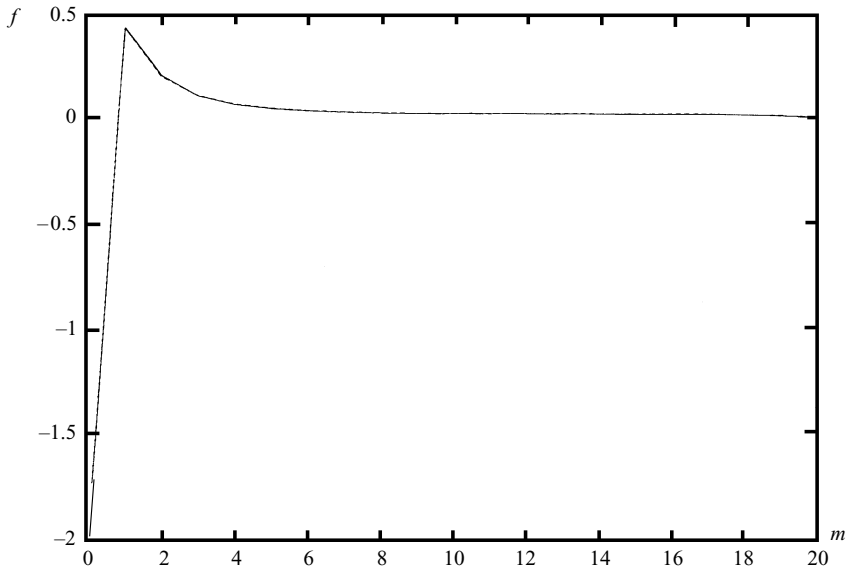

FIGURE 10. The comparison of the lattice Green's function and the kernel function; $\lambda_* = 0.58$.

The solution of the recurrence problem (40)–(42) is given by

$$\tilde{w}(t,n) = \tilde{F}(t)\,[2-\cos t - \sqrt{(3-\cos t)\,(1-\cos t)}]^n.$$

The inverse Fourier transform yields

$$w_{m,n} = \frac{1}{2\pi}\int_{-\pi}^{\pi} \tilde{w}(t,n)\,\mathrm{e}^{-imt}\,\mathrm{d}t = \frac{1}{\pi}\int_0^{\pi} [l-\sqrt{l^2-1}]^n \cos mt\,\mathrm{d}t, \tag{43}$$

where $l = 2-\cos t$. When $m \gg 1$, $n \gg 1$, it agrees with the continuum solution

$$w(x,y) = \frac{1}{\pi}\frac{y}{x^2+y^2}$$

of the Dirichlet problem in the half-plane $y > 0$.

This model uses the integer step of the discretization, and the shear stress should be specified by

$$\sigma_{23}(j,0) = \frac{\mu}{\pi}\frac{j^2-\mu_*^2}{(j^2+\lambda_*^2)^2} = \mu(w_{j,1}-w_{j,0}), \tag{44}$$

where μ is the shear modulus. Figure 10 shows that Eq. (44) holds with a high accuracy when $\lambda_* = 0.58$. Thus, the function $\mu\pi^{-1}\mathscr{K}(\xi;\mu_*,\lambda_*)$, introduced in §4, provides a very good approximation to the shear stress corresponding to the above described lattice Green's function in a half-plane. It is *not* suggested that the elementary lattice model (37)

https://doi.org/10.1017/S0956792598003489 Published online by Cambridge University Press

accurately represents an actual lattice, but the calculation nevertheless indicates the order of magnitude of λ_* which is most likely to reflect the response of an actual lattice.

6.2 Evaluation of the critical stress

6.2.1 Screw dislocation

Formally, one could use the continuum model and apply the Cottrell–Nabarro approach [16] to calculate the misfit energy and the critical shear stress σ_c required to move a screw dislocation through the lattice. For the case of an integer step in the lattice we present a summary of this calculation in the Appendix. The following equality holds:

$$\frac{\sigma_c}{\sigma_t} = 2\pi\,\mathrm{e}^{-\pi} \simeq 0.271\,521, \tag{45}$$

where $\sigma_t = \mu/(2\pi)$.

The numerical algorithm and the discrete model, developed in §4, give for a screw dislocation and an integer step of the discretization that the ratio σ_c/σ_t is located on the interval $(0.38, 0.42)$.[3] The critical stress (45) provided by Nabarro's algorithm is slightly less than these bounds. However, they have the same order of magnitude.

6.2.2 Edge dislocation

Now, we consider the case of an edge dislocation. In the frame of the continuum approach (see, for example, Hirth & Lothe [2]) the total misfit energy is equal to

$$W_m = \frac{mb}{4\pi^2}\int_{-\infty}^{\infty}\left(1+\cos\frac{2\pi\,\Phi(x)}{b}\right)\mathrm{d}x = \frac{mb^2}{4\pi(1-\nu)}. \tag{46}$$

Clearly, a shift $\Phi(x+\alpha)$ does not change the value of the misfit energy. At this point one can recall the discrete approximation of the misfit energy for an edge dislocation employed in the Peierls–Nabarro model: the integral in Eq. (46) has been approximated by an integral sum with a half-integer step of the discretization. In this case the quantity W_m depends on the shift parameter α, and $\sigma_c = \max_\alpha b^{-2}|W_m'(\alpha)|$. Formally, if one takes an arbitrary step $h \leqslant 1$ of the discretization and approximates W_m by an integral sum, then

$$\frac{\sigma_c}{\sigma_t} \sim \frac{2\pi}{(1-\nu)\,h}\,\mathrm{e}^{-\frac{\pi}{(1-\nu)\,h}}. \tag{47}$$

The value $h = 0.5$ yields Nabarro's result [4]. If we assume that the lattice calculation of the misfit energy needs the value $h = 1$, then for $\nu = 0.3$ the formula (47) yields $\sigma_c/\sigma_t \simeq 0.100\,918$. It exceeds by about 50 times the value of the normalized critical stress obtained for the case when $h = 0.5$ (see Nabarro [4]).

The parameter λ_*, evaluated for the case of anti-plane shear, can be used for an edge dislocation as well (the kernel of the integral operator differs in these two cases just by a

[3] It is consistent with simple calculations presented in the Appendix, that these values are much greater than those obtained by Nabarro [4] for an edge dislocation and a half-integer step of the discretization.

https://doi.org/10.1017/S0956792598003489 Published online by Cambridge University Press

constant factor depending on ν). The numerical algorithm (see §4) with an integer discretization step gives results, which show that the value σ_c/σ_t is located in the interval $(0.214, 0.285)$. For the modified force law (Fig. 8) this value reduces to

$$\sigma_c/\sigma_t \in (4.2\cdot 10^{-3}, 1.4\cdot 10^{-2}). \tag{48}$$

The critical stress is thus demonstrated to be highly sensitive to the form of the function F. The last estimate (48) is larger than the classical Peierls stress but we consider that this calculation may not be devoid of realism: the actual motion of a dislocation proceeds by the propagation of kinks along its length. This provides a mechanism for 'tunnelling' through the Peierls barrier, which should therefore be *expected* to exceed the critical stress that is observed.

7 Discrete model for a pair of edge dislocations of the opposite sign located on the same glide plane

This section is based on a classical example of Nabarro [4]. In accordance with the semi-continuum model, constructed for two dislocations of the opposite sign on the same glide plane, a given applied stress yields a critical separation of dislocations in unstable equilibrium.

Namely, the displacement jump Φ on the glide plane satisfies the following non-homogeneous hypersingular integral equation:

$$\sigma-(1-\nu)\sin\frac{2\pi\,\Phi}{b}=-\int_{-\infty}^{\infty}\frac{\Phi(x')}{(x-x')^2}\mathrm{d}x',\quad 0<\sigma\ll 1, \tag{49}$$

and it decays at infinity. Here σ represents the external shear stress.

Nabarro's explicit solution has the form

$$\Phi=\frac{b}{\pi}\cot^{-1}\left[\frac{(1-\nu)^2\sin\theta}{b^2}x^2-\cot\theta\right]+\frac{\theta b}{4\pi}, \tag{50}$$

which corresponds to unstable equilibrium when $\sigma=(1-\nu)\sin\theta/2$. For widely separated dislocations the parameter θ is small; it represents the shear angle at infinity. The coordinates of dislocations on the glide plane (in the state of equilibrium) are $x_{\pm}=\pm b/((1-\nu)\theta)$.

The discrete evolution model, described in previous sections, can be applied to the present example. This means that we deal with the system of nonlinear differential equations

$$\frac{\partial}{\partial t}\boldsymbol{\Phi}=\mathbf{L}\boldsymbol{\Phi}-\mathcal{N}\boldsymbol{\Phi}+\sigma\mathbf{I}. \tag{51}$$

All notations are the same as in §4 (the sinusoidal force law (2) is used for this model). We seek an even solution to (51) which decays at infinity. As in the previous section (including lattice calculations), we choose the integer discretization step ($m=1$), and $\lambda_*=0.58$. The value of the separation parameter is chosen to be $\theta=\pi/5$. The semi-continuum approach of Nabarro indicates the required value of the external shear load to be

$$(1-\nu)^{-1}\sigma\simeq 0.309, \tag{52}$$

and that the corresponding state of equilibrium is unstable. In contrast, the discrete

https://doi.org/10.1017/S0956792598003489 Published online by Cambridge University Press

lattice model gives an interval for σ associated with a stable equilibrium. In our case $(1-\nu)^{-1}\sigma \in (0.141, 0.345)$. In Fig. 11 we present contour line pictures and three-dimensional plots for the gradient region of the solution to Eq. (51). For $\sigma(1-\nu)^{-1} = 0.141$ the system of dislocations will collapse (see Fig. 11(a)). For the value $\sigma(1-\nu)^{-1} = 0.345$ the external shear stress forces the dislocations to move apart from each other (Fig. 11b)). However, as shown in Fig. 11(c), for $\sigma(1-\nu)^{-1}$ chosen inside of the above interval one has a stable equilibrium.

8 Force-velocity calculation

The evolution model (15), and its discrete analogue (21), were introduced as a mathematical device for investigating the stability of equilibrium of dislocations, and for finding an upper bound for the critical shear stress. Models of this type do, however, have some physical significance. The right sides of (15) and (21) represent the negative gradients of energy with respect to variations of the relative displacement function Φ. As such, they can be interpreted physically as forces conjugate to the state variables Φ, so Eqs. (15) and (21) represent simple kinetic equations governing the evolution of Φ with time, t. The mobility is undetermined here, and will depend on temperature; here, it is absorbed into a normalization of the time scale.

Subject to this interpretation, the plots given in Figs. 6 and 7 for σ greater than critical, provide estimates for mean velocity v of a dislocation versus σ. Figure 12 gives an example of such a plot, for the case of a discrete lattice model describing a screw dislocation, with $\lambda = 0.58$ and the integer step of discretization. When v is small we observe an apparent power law behaviour of σ versus v. It is known that for large values of v the function $\sigma(v)$ is approximately linear (see, for example, Frost & Ashby [17]). We note that Eq. (19) provides an elementary analytical model which illustrates the same phenomenon. Consider Eq. (19) with

$$\sigma > \alpha.$$

When $\alpha = 0.7$ and $\beta = 0$ the solution is illustrated in Fig. 1(a). We see a 'step-like' graph of the function $\Phi(t)$: the length of each 'step' is equal to

$$t_k - t_{k-1} = 2\pi(\sigma^2 - \alpha^2)^{-1/2}, \quad k > 0,$$

and its height is specified by

$$\Phi(t_k) - \Phi(t_{k-1}) = 2\pi.$$

The 'average velocity' is defined to be

$$v = \frac{\Phi(t_k) - \Phi(t_{k-1})}{t_k - t_{k-1}} = \sqrt{\sigma^2 - \alpha^2}. \tag{53}$$

The graphs of σ versus v are presented in Figs. 1(b), (c). It follows from Eq. (53) that, when $\sigma \gg 1$

$$\sigma \sim v.$$

On the other hand, if $0 < \sigma - \alpha \ll 1$ then

$$\sigma \sim (2\alpha)^{-1} v^2 + \alpha.$$

https://doi.org/10.1017/S0956792598003489 Published online by Cambridge University Press

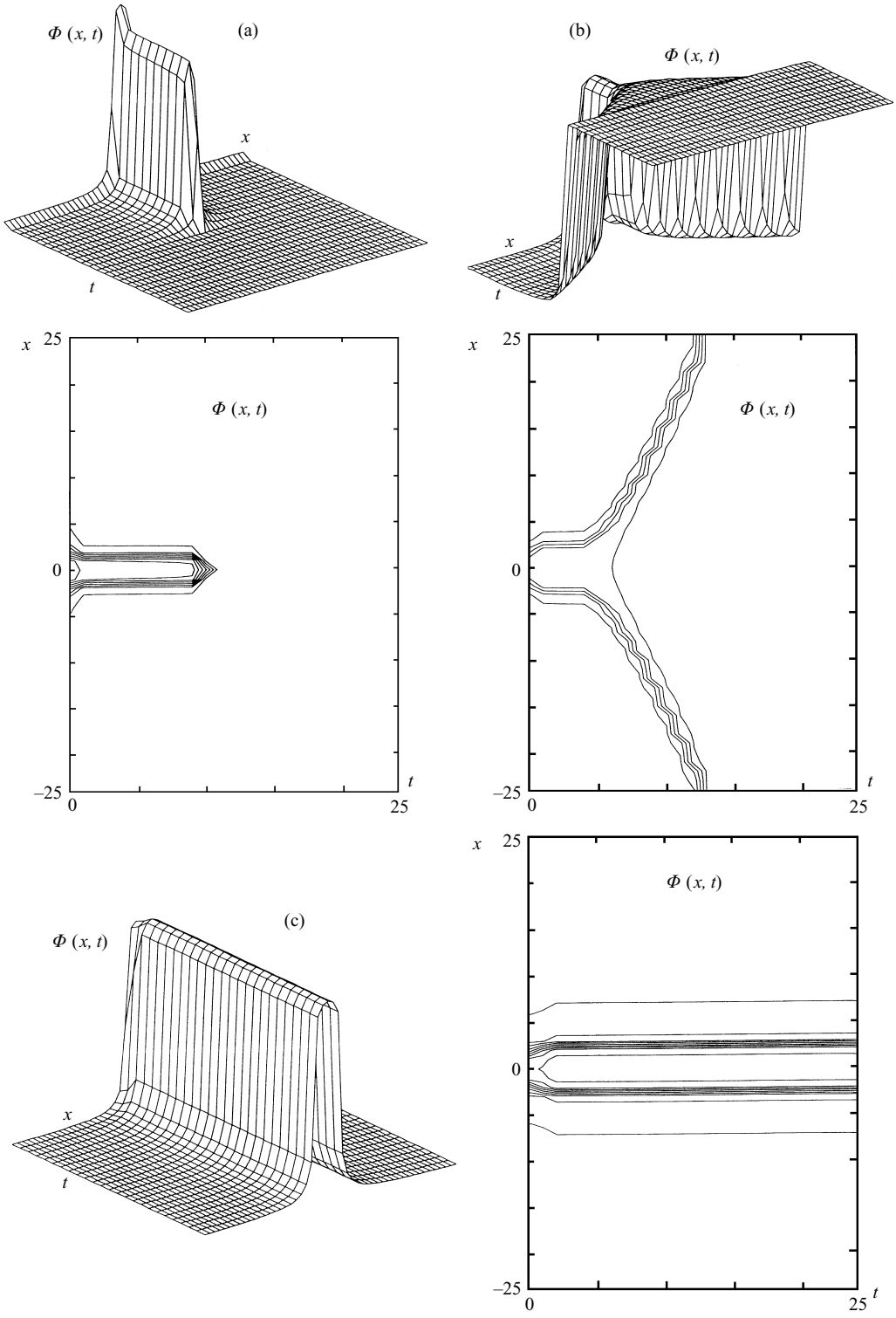

FIGURE 11. The contour line pictures for the displacement jump on the glide plane containing two edge dislocations of opposite sign; $\lambda_* = 0.58$, $m = 1$, $\nu = 0.3$. (a) $\sigma(1-\nu)^{-1} = 0.141$; (b) $\sigma(1-\nu)^{-1} = 0.345$; (c) $\sigma(1-\nu)^{-1} = 0.309$.

https://doi.org/10.1017/S0956792598003489 Published online by Cambridge University Press

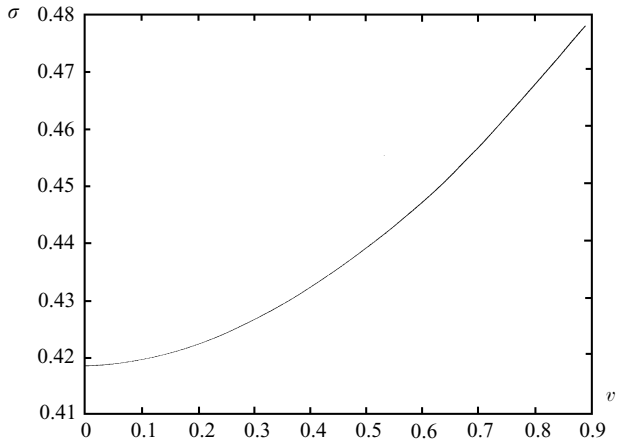

FIGURE 12. The graph of σ versus v obtained for the case of a screw dislocation (discrete model) with the integer step of discretization and $\lambda_* = 0.58$.

It shows explicitly the power law behaviour of $\sigma(v)$ for small values of the average velocity (compare with the graph in Fig. 1(b)), and the linear dependence on v for the case when $\sigma \gg 1$ (see Fig. 1(c)).

9 Conclusion

A discrete nonlinear model for edge and screw dislocations has been developed. We have shown that the semi-continuum model for a nonhomogeneous Peierls equation is not appropriate for calculation of the critical shear stress required to move the dislocation through the discrete lattice. In accordance with the lattice model we presented the stability analysis for the evolution system of nonlinear differential equations. For two different types of the interatomic force law we obtained upper and lower bounds for the critical shear load. The value of the Peierls stress is slightly smaller than one predicted by our model, but those values have the same order of magnitude. Analysis of a lattice Green's function enabled us to choose the appropriate regularization parameter λ_* for the kernel of the singular operator of the convolution type. Also, the discrete model has been applied to a pair of edge dislocations of the opposite sign located on the same glide plane. We have obtained the interval for values of external shear stress which provide a stable equilibrium of this discrete system.

Acknowledgements

The authors acknowledge the valuable suggestions of the referee. Also, we would like to thank Drs S. D. Howison and J. R. Ockendon for their comments.

Appendix

This appendix includes the calculations mentioned in §6.2 of the main text. Here we follow the Cottrell–Nabarro scheme [16] and present the discrete approximation of the misfit

energy integral W_m for an integer discretization parameter for the case of a screw dislocation:

$$W_m(x) = \frac{\mu b^2}{4\pi^2} \sum_{n=-\infty}^{\infty} [1+\cos 2\{\tan^{-1} 2(n+\alpha)\}]$$

$$= \frac{\mu b^2}{2\pi^2} \sum_{n=-\infty}^{\infty} \frac{1}{1+4(n+\alpha)^2}.$$

The last sum can be represented by

$$\frac{\mu b^2}{8\pi^2} \sum_{n=-\infty}^{\infty} \frac{1}{q^2+(n+p)^2} \simeq \frac{\mu b^2}{8\pi^2} \left\{ \frac{\pi}{q} + \frac{2\pi}{q} e^{-2q\pi} \cos(2p\pi) + \cdots \right\},$$

where $p = \alpha$, $q = 1/2$. Then

$$\sigma_c = \max_a \left| \frac{1}{b^2} \frac{dW_m}{d\alpha} \right| \simeq \mu e^{-\pi},$$

and

$$\frac{\sigma_c}{\sigma_t} = 2\pi e^{-\pi} \simeq 0.271\,521.$$

References

[1] Taylor, G. I. (1934) The mechanism of plastic deformation of crystals. Part I. Theoretical. *Proc. Royal Soc. A*, **145**, 362–404.

[2] Hirth, J. P. & Lothe, J. (1968) *Theory of Dislocations*. McGraw-Hill.

[3] Peierls, R. E. (1940) The size of a dislocation. *Proc. Phys. Soc.* **52**, 34–37.

[4] Nabarro, F. R. N. (1947) Dislocations in a simple cubic lattice. *Proc. Phys. Soc.* **59**, 256–272.

[5] Foreman, B. J., Jaswon, M. A. & Wood, J. K. (1951) Factors controlling dislocation widths. *Proc. Phys. Soc. A* **64**, 156–163.

[6] Bullough, R., Movchan, A. B. & Willis, J. R. (1991) The Peierls stress for various dislocation morphologies. *Materials Modelling: From Theory to Technology*, Oxford, pp. 73–78.

[7] Frenkel, J. & Kontorova, T. (1938) On the theory of plastic deformation and twinning. *J. Phys. USSR* **13**, 1–10.

[8] Hobart, R. (1965) Peierls stress dependence on dislocation width. *J. Appl. Phys.* **36**, 1944–1948.

[9] Lomdahl, P. S. & Srolovitz, D. J. (1986) Dislocation generation in the two-dimensional Frenkel–Kontorova model at high stress. *Phys. Rev. Lett.* **57**, 2702–2705.

[10] Vitek, V., Perrin, R. C. & Bowen, D. K. (1970) The core structure of screw dislocations in b.c.c. crystals. *Phil. Mag.* **21**, 1049–1073.

[11] Bazinski, Z. S., Duesbery, M. S. & Taylor, R. (1970) Screw dislocations in a model sodium lattice. *Phil. Mag.* **21**, 1201–1221.

[12] Bazinski, Z. S., Duesbery, M. S. & Taylor, R. (1970) Influence of shear stress on screw dislocations in a model sodium lattice. *Canadian J. Phys.* **49**, 2160–2180.

[13] Carpio, A., Chapman, S. J., Howison, S. D. & Ockendon, J. R. (1997) Dynamics of line singularities. *Phil. Trans.* **355**(1731), 2013–2024.

[14] Debye, P. (1912) Zur theorie der spezifischen wärmen. *Annalen der Physik* **39**, 789–839.

[15] Carr, J. (1981) *Applications of Centre Manifold Theory*. Springer-Verlag, New York.

[16] Cottrell, A. H. (1952) *Dislocations and Plastic Flow in Crystals*. Oxford.

[17] Frost, H. F. & Ashby, M. F. (1982) *Deformation-mechanism maps: The plasticity and creep of metals and ceramics*. Pergamon, Oxford.